

Effect of Ferrosilicon Alloys on the Composition of Inclusions in Austenitic Stainless Steel Melts

J. H. Park*

ABSTRACT

The silicon deoxidation equilibrium between the 16Cr-14Ni-1.5Mn-Si melts and the CaO-SiO₂-8MgO-5CaF₂ (basicity=1.8) slag at 1743 K was investigated to understand the effect of aluminum and silicon contents on the composition of inclusions. Therefore, the ferrosilicon alloys with different aluminum content were chosen based on the above objective. In addition, the phase stability diagram of the inclusions was computed using commercial thermodynamic software based on the Gibbs energy minimization principles. The content of MnO in the inclusions sharply decreases with increasing silicon content when the steel melts were deoxidized by the ferrosilicon alloys containing high aluminum (FeSi-H). The content of SiO₂ in the inclusions slightly increases with increasing silicon content when the FeSi-L was used, while a maximum value is shown at [Si]=1.5mass% when the FeSi-H was used. The content of MgO in the inclusions increases by increasing the content of silicon, regardless of the kinds of ferrosilicon alloys. The use of the FeSi-L as a deoxidizer could suppress the formation of Al₂O₃ in the inclusions, while the content of Al₂O₃ increases with increasing silicon content when the FeSi-H was used. When the FeSi-H was used as a deoxidizer, the inclusions are the glassy-type with the composition of Mn-silicates at [Si] 1.3mass%, while the Mg(Ca)-silicates with the composition of the forsterite phase is observed in the steel composition of [Si]=3.3mass%. When the steel melts were deoxidized by the FeSi-L alloys, the inclusions are the glassy-type Mn-silicates at [Si]=0.8mass%, while the Mn-silicates containing the cristobalite phase are observed at [Si]=1.5 to 2.4mass%. In the composition of [Si]=3.3mass%, the Mg-silicates with the composition of the rhodonite phase are observed.

Key words : silicon deoxidation, inclusion, ferrosilicon, phase stability diagram, thermodynamics.

1. Introduction

Austenitic stainless steel melts have generally been deoxidized by addition of ferrosilicon alloys in the argon oxygen decarburization converter. The silicon deoxidation equilibrium and the composition of inclusions in type 304 (18 mass pct Cr-8 mass pct Ni) stainless steel melts have widely been reported by many

researchers.^[1-6] However, recently, the use of austenitic stainless steels has been broaden to the fields of the electronic assembly as well as the exhaust manifold system. This means that the alloying elements such as nickel and silicon are needed to satisfy the required performance, for example good formability and oxidation resistance at elevated temperatures. Because these properties are generally affected by the type of inclusions in the materials, the information of the inclusions formed during steelmaking and casting processes should be

* Stainless Steel Research Group

understood. Several studies regarding the composition and morphology of inclusions in the austenitic stainless steel melts are reviewed as follows.

Kim *et al.* reported that the spinel (MgAl_2O_4) phase could be crystallized in the suspended $\text{CaO-SiO}_2\text{-MgO-Al}_2\text{O}_3$ ($-\text{TiO}_2$) inclusion matrix as the temperature of molten steel (type 304) decreased from about 1923 K at AOD converter to about 1723 K at continuous casting mold.^[2] From the analysis of plant data, they proposed that the aluminum content in steel melt and MgO content in AOD slag should be lowered to suppress the formation of spinel. The crystallization of spinel in the liquid $\text{CaO-SiO}_2\text{-MgO-Al}_2\text{O}_3$ inclusion matrix, with Al_2O_3 content greater than about 20 mass pct, has also recently been reported by Ehara *et al.*^[5] However, the thermodynamic analysis regarding the deoxidation equilibrium is not available in these works.

Nishi and Shinme observed that the content of MgO in the alumina-based inclusions, readily formed by aluminum deoxidation of type 304 stainless steel, increased with increasing basicity ((mass pct CaO)/(mass pct SiO_2)) of the $\text{CaO-SiO}_2\text{-MgO-Al}_2\text{O}_3$ slags.^[7] They proposed that the reduction of MgO in the slag by aluminum in molten steel at the slag/metal interface would provide small amounts of magnesium, which could react with Al_2O_3 inclusions, *albeit* less than 1 mass ppm magnesium. The similar mechanism was suggested by Todoroki *et al.*^[3, 8] Furthermore, they observed that the SiO_2 in the slag enhanced the stability of the spinel inclusion in type 304 stainless steel melts.^[9] Although the content of aluminum in molten steel was from about 0.01 to 1 mass pct in these studies, only the reduction of MgO (or CaO) was considered. However, the SiO_2 could also be reduced by such a large content of aluminum, which was not taken into account.

The effect of aluminum and calcium in the ferrosilicon alloys on the inclusion formation after the silicon deoxidation of type 304 stainless steel was significantly studied by Todoroki *et*

al.^[3] The aluminum in the ferrosilicon alloys was found to reduce MgO in the slags, resulting in the formation of spinel inclusion, while the calcium was found to prevent the formation of spinel and to form the calcium silicate inclusions with relatively low melting point. Tanahashi *et al.* calculated that the composition of inclusions in type 304 stainless steel melts could be changed in the order of “ MnCr_2O_4 $\text{MnCr}_2\text{O}_4\text{+Mn-silicate}$ Mn-silicate Mn-silicate+SiO_2 SiO_2 ” by increasing the content of silicon to about 2 pct.^[6] However, the effect of impurity element such as aluminum in the silicon deoxidation process could not be taken into account in this work.

Therefore, in the present study, the silicon deoxidation equilibrium between the 16 mass pct Cr-14 mass pct Ni-1.5 mass pct Mn-Si melts and the $\text{CaO-SiO}_2\text{-8 mass pct MgO-5 mass pct CaF}_2$ slag (basicity=1.8) was investigated to understand the effect of aluminum and silicon contents on the composition of inclusions. Here, the ferrosilicon alloys with different aluminum content were chosen based on the above purpose. In addition, the phase stability diagram of the inclusions was computed using commercial thermodynamic software based on the Gibbs energy minimization principles.

2. Experimental

The pure iron, chromium, nickel, and manganese were premelted in a vacuum induction furnace to make a composition of Fe-16 mass pct Cr-14 mass pct Ni-1.5 mass pct Mn stainless steel. The metal samples of about 330 grams and the $\text{CaO-SiO}_2\text{-8 mass pct MgO-5 mass pct CaF}_2$ (B=1.8) slags of about 7 grams were equilibrated in the pure MgO crucibles, which were located in a high frequency induction furnace. The initial content of aluminum in the premelted Fe-16 pct Cr-14 pct Ni-1.5 pct Mn steel was less than about 20 ppm. The amount of ferrosilicon alloys was changed to control the content of silicon in the melt from

about 0.8 to 3.3 mass pct. The compositions of ferrosilicon alloys (FeSi-H and FeSi-L) used in this study are listed in Table 1.

Table 1. Composition of the Ferrosilicon Alloys used in This Study as a Deoxidizer.

	[pct Si]	[pct Al]	[pct Fe]
FeSi-H	76.6	1.13	22.0
FeSi-L	76.3	0.17	23.5

A schematic diagram of the experimental apparatus is shown in Fig. 1 and the experimental temperature was controlled to be 1873 and 1743 (± 3) K using an R-type (Pt-13 mass pct Rh/Pt) thermocouple and a proportional integral differential controller. The oxygen as an impurity in an Ar gas was removed by passing the gas through magnesium turnings heated to about 773 K. After the steel samples were melted at 1873 K, the ferrosilicon alloys were added, followed by the addition of the premelted slags with the composition of the Ca_2SiO_4 saturation condition at 1873 K.^[10] Then, the system was cooled to 1743 K and was equilibrated during 30 minutes, which was preliminarily determined.

After equilibrating, the power of the furnace was off and the crucible assembly was quenched by Ar gas. The metal and slag samples were prepared for chemical analysis. The steel compositions were analyzed by an optical emission spectroscope and the content of total oxygen was determined by fusion and the infrared absorption method. The composition of the slags was analyzed by an X-ray fluorescence spectrometer. The samples were mounted in cold-setting resin. Standard grinding and polishing techniques then were used, after which all samples were gold coated. Finally, the composition and the morphology of about ten inclusions per sample were examined by backscattered electron imaging (BEI) using a SEM-EDS (model JSM-840A, JEOL,^{*}) with a link detector.

* JEOL is a trademark of Japan Electron Optics Ltd., Tokyo.

The composition of the inclusions in a specific run was taken from the average value of about ten inclusions. The equilibrium compositions of the metal samples after experiments are listed in Table 2.

Table 2. Composition of the Stainless Steel Melts Before and After Equilibrium at 1743 K.

Heat No.	@ 1873K		@ 1743K		
	[pct Si] ^o	[pct Al] ^o	[pct Si]	[pct Al] ^{dissolved}	[pct O] ^{total}
FSH-1	0.8	0.0040	0.7	0.0013	0.0052
FSH-2	1.5	0.0142	1.2	0.0013	0.0047
FSH-3	2.4	0.0278	2.1	0.0013	0.0047
FSH-4	3.3	0.0415	2.9	0.0016	0.0031
FSL-1	0.8	0.0006	0.7	0.0012	0.0041
FSL-2	1.5	0.0022	1.3	0.0011	0.0033
FSL-3	2.4	0.0042	2.1	0.0009	0.0033
FSL-4	3.3	0.0062	3.0	0.0009	0.0014

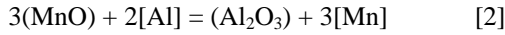
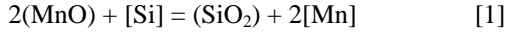
Moreover, a phase stability diagram of the inclusions was calculated using commercial thermodynamic software, FactSage 5.3.1TM along with FToxid53 and FTmisc databases, on the basis of the Gibbs energy minimization principles.^[11]

3. Results and Discussion

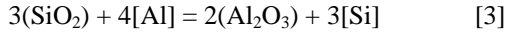
3.1 Composition Changes of Inclusions in Fe-16Cr-14Ni-Si Melts Equilibrated with CaO-SiO₂-8MgO-5CaF₂ (B=1.8) Slags

The contents of MnO, SiO₂, MgO, and Al₂O₃ in the inclusions are shown in Fig. 2 (a) and (b) as a function of the initial content of silicon in the Fe-16 mass pct Cr-14 mass pct Ni-1.5 mass pct Mn-Si melts equilibrated with the CaO-SiO₂-8 mass pct MgO-5 mass pct CaF₂ (B=1.8) slag at 1743 K. The content of MnO decreases from about 45 to 20 mass pct with increasing silicon content from 0.8 to 3.3 mass pct when the steel melts were deoxidized by the ferrosilicon alloys containing the relatively low content of

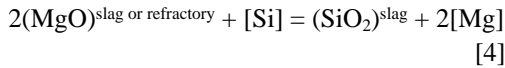
aluminum (FeSi-L). The content of MnO in the inclusions sharply decreases from about 45 to 5 mass pct by increasing the content of silicon when the steel melts were deoxidized by the ferrosilicon alloys containing the relatively high content of aluminum (FeSi-H). This is simply due to the reduction of MnO in the inclusions by silicon (Eq. [1]) and especially by silicon and aluminum (Eq. [2]) in the latter case.



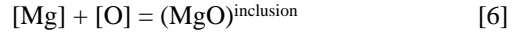
The content of SiO_2 in the inclusions slightly increases from about 40 to 55 mass pct with increasing silicon content when the FeSi-L was used, while a maximum value is shown at $[\text{Si}] = 1.5$ mass pct when the FeSi-H was used. In this case, the partial reduction of SiO_2 in the inclusions by aluminum (Eq. [3]) could be expected in the composition of silicon content greater than 1.5 mass pct.



In Fig. 2 (b), the content of MgO in the inclusions increases from about 5 to 20 mass pct by increasing the content of silicon, regardless of the kinds of ferrosilicon alloys. It is of interest that the content of MgO in the inclusions when the FeSi-L was added is greater than that of MgO when the FeSi-H was added in the Fe-16 pct Cr-14 pct Ni-1.5 pct Mn-3.3 pct Si melts. This means that the magnesium, which is transferred from the slag (or refractory) / metal interface by the reaction between MgO and Si (Eq. [4]),^[12] could participate in deoxidation (Eq. [6]) processes in the high silicon stainless steel melts.^[13]



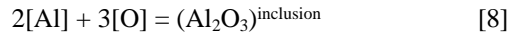
$$\log K_{[4]} = \log \left[\frac{a_{\text{SiO}_2} \cdot a_{\text{Mg}}^2}{a_{\text{MgO}}^2 \cdot a_{\text{Si}}} \right] = \frac{15200}{T} - 16.96 \quad [5]$$



$$\log K_{[6]} = \log \left[\frac{a_{\text{MgO}}}{a_{\text{Mg}} \cdot a_{\text{O}}} \right] = \frac{4700}{T} + 4.28 \quad [7]$$

where $K_{[n]}$, a_{MO} , and a_{M} are, respectively, the equilibrium constant of Eq. [n], the activity of MO in the oxide phase, and the activity of M in the steel melt, of which standard state is the infinite dilute solution.

Finally, the use of the FeSi-L as a deoxidizer could suppress the formation of Al_2O_3 in the inclusions, while the content of Al_2O_3 increases up to about 15 mass pct with increasing silicon content up to about 3.3 mass pct when the FeSi-H was used. This could be resulted from the Eqs. [2], [3], and [8].^[14]



$$\log K_{[8]} = \frac{45300}{T} - 11.62 \quad [9]$$

The changes in the composition of the inclusions when the steel melts were deoxidized by the FeSi-H are shown in Fig. 3 by using the MnO-SiO₂-MgO and MgO-SiO₂-Al₂O₃ phase diagrams.^[15] The inclusions in the steel melts, with the composition of silicon content less than about 2.4 mass pct (H₁ to H₃), are the homogeneous liquid phase at 1743 K. However, the forsterite (Mg_2SiO_4 , or olivine) inclusions containing small amounts of MnO as well as Al_2O_3 could be formed in the Fe-16 pct Cr-14 pct Ni-1.5 pct Mn-3.3 pct Si melts (H₄) at 1743 K. The representative morphology and mean composition of the inclusions when the steel melts were deoxidized by the FeSi-H are appeared in Fig. 4. The inclusions are the glassy-type with the composition of Mn-silicates in the silicon content less than about 1.3 mass pct (H₁ and H₂), while the Mg(Ca)-silicates with the composition of the forsterite (or olivine) phase is observed in the silicon content about 3.3 mass pct (H₄).

The changes in the composition of the inclusions when the steel melts were deoxidized by the FeSi-L are shown in Fig. 5. The inclusions in the steel melt of [Si]=0.8 mass pct (L_1) is the homogeneous liquid phase at 1743 K. However, the inclusions containing the cristobalite (SiO_2) phase are observed in the steel melts of the silicon content up to about 2.4 mass pct (L_2 and L_3). Finally, the rhodonite ($(\text{Mg}, \text{Mn})\text{SiO}_3$) inclusions could be formed in the Fe-16 pct Cr-14 pct Ni-1.5 pct Mn-3.3 pct Si melts (L_4) at 1743 K. The representative morphology and mean composition of the inclusions when the steel melts were deoxidized by the FeSi-L are appeared in Fig. 6. The L_1 inclusions are the glassy-type with the composition of Mn-silicates, while the L_2 and L_3 inclusions are the Mn-silicates containing the cristobalite phase. The L_4 inclusions are the Mg-silicates with the composition of the rhodonite phase from the phase diagram of the MgO-SiO₂-MnO system.

In the present study, a phase stability diagram of the inclusions in the Fe-16 pct Cr-14 pct Ni-1.5 pct Mn-0.001 pct Al-0.006 pct O-Si-Mg melts at 1743K was also calculated using FactSage thermodynamic software.^[11] In the calculations, FToxid53 database for all oxide phases and FTmisc database for molten steel were employed. Since the top slag and the liquid oxide inclusions are represented as one solution in the database, it is difficult to directly calculate the phase equilibria among top slag, molten steel, and liquid inclusions. Therefore, in the present calculations, the following procedure was used.

Firstly, 350 grams of steel (Fe-16 pct Cr-14 pct Ni-1.5 pct Mn) and 7 grams of slag with the same composition of the experiment were equilibrated at 1873 K with additions of the FeSi-H or FeSi-L alloys, whose compositions are also given in Table 1. This calculation could simulate how much magnesium could be reduced from the top slag containing MgO by the FeSi alloys. From these calculations, the reduced magnesium contents in the molten steel can be obtained as a function of the initial

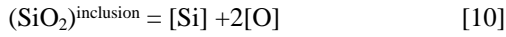
content of silicon in the steel melts. Secondly, a phase stability diagram of the inclusions in the Fe-16 pct Cr-14 pct Ni-1.5 pct Mn-0.001 pct Al-0.006 pct O-Si-Mg melts at 1743 K was calculated without further considering the top slag. This phase stability diagram is shown in Fig. 7 with the previously calculated magnesium content in the steel melts as a function of silicon content. If it is assumed that the reduced magnesium in the steel melts is preserved from 1873 K to 1743 K during cooling and participate in deoxidation reaction at 1743 K, the calculated two lines in Fig. 7 may represent the stable inclusion phases in equilibrium with molten steel.

There are complicated phases as a function of each element, such as “Spinel Mg-Mn-Si-Al-O liquid oxide” as the silicon content increases at magnesium content less than about 10 ppm. The inclusions could change in the order of “Spinel + Olivine (mainly Mg_2SiO_4 (forsterite))

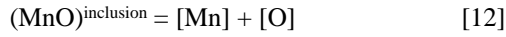
Olivine + Mg-Mn-Si-Al-O liquid oxide” by increasing the content of silicon at magnesium content from about 10 to 30 mass ppm. The content of magnesium increases from about 8 to 30 ppm with increasing silicon content, indicating the reduction reaction of MgO by silicon as described in Eq. [4]. The formation of olivine and liquid inclusion can qualitatively be expected, while that of spinel at the relatively low magnesium and silicon content region is different from the observed results. Although the reason for this discrepancy is not fully understood yet, it is suggested that there are some regions in the thermodynamic databases to be improved for the highly alloyed melts such as stainless steel.

3.2 Thermodynamic Equilibria between Inclusions and Fe-16Cr-14Ni-Si Melts

The formation of the Mn-silicate inclusions can be discussed based on the thermodynamic equilibrium with silicon, manganese, and oxygen in the steel melts as follows:



$$a_{\text{SiO}_2} = \frac{a_{\text{Si}} \cdot a_{\text{O}}^2}{K_{\text{Si}}} \quad [11]$$



$$a_{\text{MnO}} = \frac{a_{\text{Mn}} \cdot a_{\text{O}}}{K_{\text{Mn}}} \quad [13]$$

where a_M is the activity of M, and K_{Si} and K_{Mn} are, respectively, the equilibrium constant of Eqs. [10] and [12]. By combining Eqs. [11] and [13], the composition of the inclusions can be deduced as a function of the activities of silicon, manganese, and oxygen as follows:

$$\log\left(\frac{X_{\text{SiO}_2}}{X_{\text{MnO}}}\right) = \log\left[\frac{a_{\text{Si}} \cdot a_{\text{O}}}{a_{\text{Mn}}}\right] - \log\left(\frac{\gamma_{\text{SiO}_2}}{\gamma_{\text{MnO}}}\right) + \log\left[\frac{K_{\text{Mn}}}{K_{\text{Si}}}\right] \quad [14]$$

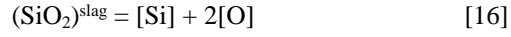
where X_{MO} and γ_{MO} are the mole fraction and the activity coefficient of MO in the inclusions. Hence, the ratio of SiO_2 to MnO of inclusions, $\log(X_{\text{SiO}_2} / X_{\text{MnO}})$, is expected to exhibit a linear relation to the $\log[a_{\text{Si}} \cdot a_{\text{O}} / a_{\text{Mn}}]$ with the slope of unity at a fixed temperature, if the activity coefficient term would not significantly be affected by steel compositions.

The ratio of X_{SiO_2} to X_{MnO} of the inclusions in the Fe-16 pct Cr-14 pct Ni-1.5 pct Mn-Si stainless steel melts equilibrated with the CaO-SiO₂-8 pct MgO-5 pct CaF₂ (B=1.8) slag at 1743 K is shown in Fig. 8 as a function of the ratio of $a_{\text{Si}} \cdot a_{\text{O}}$ to a_{Mn} in logarithmic scale. Here, the activities of silicon and manganese (M) were calculated by Eq. [15].

$$\begin{aligned} \log a_M &= \log f_M + \log[\text{pct } M] \\ &= \sum_{i=\text{Cr, Ni, Al, Si, Mn}} (e_M^i \cdot [\text{pct } i]) + \log[\text{pct } M] \quad [15] \end{aligned}$$

where f_M and e are, respectively, the activity coefficient of silicon and manganese in molten

steel, and the interaction parameters, which are listed in Table 3.^[16-19] Also, the activity of oxygen in the steel melts could be calculated from the slag/metal (Si-O deoxidation) equilibrium reaction as shown in Eq. [16].^[17]



$$\log K_{[16]} = \frac{24600}{T} + 8.4 \quad [17]$$

Table 3. Interaction Parameters Employed in This Study.

e_i^j	Cr	Ni	Al	Si	Mn
Si	-0.021 ^[17]	-0.009 ^[17]	0.058	0.103	-
Mn	0.0039 ^[19]	-0.0085 ^[19]	0.071 ⁺	-1838/T+0.964	0.0

+calculated from $e_{\text{Al}}^{\text{Mn}} (=0.035)$ ^[20]

In the composition of the steel melts investigated in this study, the $\log(X_{\text{SiO}_2} / X_{\text{MnO}})$ of the inclusions linearly increases by increasing the $\log[a_{\text{Si}} \cdot a_{\text{O}} / a_{\text{Mn}}]$. However, it is of interest that the slope of the line is about 0.9 when the FeSi-L was used as a deoxidizer, while the slope of the line is about 2.0, which is greater than that of the expected value of unity in Eq. [14] when the FeSi-H was used. In this case, it is expected that the activity coefficient term, $(\gamma_{\text{SiO}_2} / \gamma_{\text{MnO}})$, in Eq. [14] could be decreased as the composition of steel melts changes to the relatively high silicon activity region. This is qualitatively in accordance with the experimental results shown in Figs. 2 and 4, which indicate that the content of Al_2O_3 increases with increasing silicon content due to aluminum inevitably came from the FeSi-H alloys. Actually, the value of γ_{MnO} would not significantly be changed with increasing Al_2O_3 content, while the value of γ_{MnO} decreases with increasing Al_2O_3 content, if the ratio of MnO to SiO_2 would not significantly be changed from the thermodynamic data for the MnO-SiO₂-Al₂O₃ system, which were reported by Ohta and Suito.^[20]

On the other hand, the content of MgO in the inclusions, investigated in the present study, increased with increasing silicon content as

discussed in section A (Eqs. [4] and [6]). Thus, the thermodynamic equilibrium with magnesium, manganese, and oxygen in the steel melts should be taken into account to understand the changes of the MgO/MnO ratio in the silicate inclusions. The correlations between the ratio of X_{MgO} to X_{MnO} in the inclusions and the ratio of a_{Mg} to a_{Mn} in the steel melts could be deduced as follows from Eqs. [7] and [13].

$$\log\left(\frac{X_{\text{MgO}}}{X_{\text{MnO}}}\right) = \log\left[\frac{a_{\text{Mg}}}{a_{\text{Mn}}}\right] - \log\left(\frac{\gamma_{\text{MgO}}}{\gamma_{\text{MnO}}}\right) + \log\left[\frac{K_{\text{Mn}}}{K_{\text{Mg}}}\right] \quad [18]$$

Hence, the ratio of MgO to MnO of the inclusions, $\log(X_{\text{MgO}} / X_{\text{MnO}})$, is expected to exhibit a linear relation to the $\log[a_{\text{Mg}} / a_{\text{Mn}}]$ with the slope of unity at a fixed temperature, if the activity coefficient term would not significantly be affected by steel compositions.

The ratio of X_{MgO} to X_{MnO} of the inclusions in the Fe-16 pct Cr-14 pct Ni-1.5 pct Mn-Si stainless steel melts equilibrated with the CaO-SiO₂-8 pct MgO-5 pct CaF₂ (B=1.8) slag at 1743 K is shown in Fig. 9 as a function of the ratio of a_{Mg} to a_{Mn} in logarithmic scale. Here, the activity of magnesium in the steel melts could be calculated from the slag/metal equilibrium reaction (Eq. [4]).

In the composition of the steel melts investigated in this study, the $\log(X_{\text{MgO}} / X_{\text{MnO}})$ of the inclusions linearly increases by increasing the $\log[a_{\text{Mg}} / a_{\text{Mn}}]$ with the slopes of about 2.1 and 3.0 in the cases of the use of FeSi-L and FeSi-H as a deoxidizer, respectively. Hence, it is expected that the activity coefficient term, $(\gamma_{\text{MgO}} / \gamma_{\text{MnO}})$ in the silicate inclusions, in Eq. [18] could be decreased as the composition of the steel melts changes to the relatively high magnesium activity region. Actually, the value of γ_{MnO} increases by increasing the value of $X_{\text{MgO}} / X_{\text{MnO}}$ ratio, if the content of SiO₂ would not significantly be changed, from the

thermodynamic data for the MgO-MnO-SiO₂ system, although the activity coefficient of MgO in this system is not available.^[21]

4. Conclusions

The silicon deoxidation equilibrium between the 16 mass pct Cr-14 mass pct Ni-1.5 mass pct Mn-Si melts and the CaO-SiO₂-8 mass pct MgO-5 mass pct CaF₂ (basicity=1.8) slag at 1743 K was investigated to understand the effect of aluminum and silicon contents on the composition of inclusions. Therefore, the ferrosilicon alloys with different aluminum content were chosen based on the above objective. In addition, the phase stability diagram of the inclusions was computed using commercial thermodynamic software based on the Gibbs energy minimization principles. The following conclusions were obtained:

- 1) The content of MnO in the inclusions decreases with increasing silicon content when the steel melts were deoxidized by the ferrosilicon alloys. This trend is more significant when the ferrosilicon alloys containing high aluminum (FeSi-H) was used. The content of SiO₂ in the inclusions slightly increases with increasing silicon content when the FeSi-L was used, while a maximum value is shown at [Si]=1.5 mass pct when the FeSi-H was used.
- 2) The content of MgO in the inclusions increases by increasing the content of silicon, regardless of the kinds of ferrosilicon alloys. The use of the FeSi-L as a deoxidizer could suppress the formation of Al₂O₃ in the inclusions, while the content of Al₂O₃ increases with increasing silicon content when the FeSi-H was used.
- 3) When the FeSi-H was used as a deoxidizer, the inclusions are the glassy-type with the composition of Mn-silicates at [Si] 1.3 mass pct, while the Mg(Ca)-silicates with the composition of the forsterite phase is observed in the steel composition of [Si]=3.3 mass pct.

- 4) When the steel melts were deoxidized by the FeSi-L alloys, the inclusions are the glassy-type Mn-silicates at [Si]=0.8 mass pct, while the Mn-silicates containing the cristobalite phase are observed at [Si]=1.5 to 2.4 mass pct. In the composition of [Si]=3.3 mass pct, the Mg-silicates with the composition of the rhodonite phase are observed.
- 5) In the composition of the steel melts investigated in this study, the $\log(X_{\text{SiO}_2} / X_{\text{MnO}})$ of the inclusions linearly increases by increasing the $\log [a_{\text{Si}} \cdot a_{\text{O}} / a_{\text{Mn}}]$ with the slope close to unity, when the FeSi-L was used as a deoxidizer, while the slope of the line is about two times greater than that of the expected value when the FeSi-H was used.
- 6) The $\log(X_{\text{MgO}} / X_{\text{MnO}})$ of the inclusions linearly increases by increasing the $\log [a_{\text{Mg}} / a_{\text{Mn}}]$ with the slopes of about 2.1 and 3.0, which are greater than the expected value of unity, in the cases of the use of FeSi-L and FeSi-H as a deoxidizer, respectively.

References

- (1) Y. Hayashi, M. Kanno, H. Yoshida, S. Inada, T. Kawahara, and S. Ono: *Proc. 6th Int. Iron Steel Congr.*, Nagoya, Oct. 21-26, 1990, ISIJ, Tokyo, 1990, vol. 3, pp. 551-57.
- (2) J.W. Kim, S.K. Kim, D.S. Kim, Y.D. Lee, and P.K. Yang: *Iron Steel Inst. Jpn. Int.*, 1996, vol. 36, pp. S140-43.
- (3) H. Todoroki, K. Mizuno, M. Noda, T. Tohge: *2001 Steelmaking Conf. Proc.*, Baltimore, MD, Mar. 25-28, 2001, ISS-AAIME, Warrendale, PA, 2001, pp. 331-41.
- (4) K. Suzuki, S. Ban-ya, and M. Hino: *Iron Steel Inst. Jpn. Int.*, 2002, vol. 42, pp. 146-49.
- (5) Y. Ehara, S. Nakamura, and Y. Habara: *Proc. 4th Eur. Stainless Steel Science and Market Cong.*, Paris, Jun. 10-13 (2002), ATS, Paris, 2002, vol. 2, pp. 176-81.
- (6) M. Tanahashi, T. Taniguchi, T. Kayukawa, C. Yamauchi, and T. Fujisawa: *Tetsu-to-Hagané*, 2003, vol. 89, pp. 1183-90.
- (7) T. Nishi and K. Shinme: *Tetsu-to-Tagané*, 1998, vol. 84, pp. 837-43.
- (8) H. Todoroki and K. Mizuno: *Trans. ISS*, 2003, Mar., pp. 60-67.
- (9) H. Todoroki and K. Mizuno: *Iron Steel Inst. Jpn. Int.*, 2004, vol. 44, pp. 1350-57.
- (10) C.H. Choi, S.K. Jo, S.H. Kim, K.R. Lee, and J.T. Kim: *Metall. Mater. Trans. B*, 2004, vol. 35B, pp. 115-20.
- (11) C.W. Bale, P. Chartrand, S.A. Decterov, G. Eriksson, K. Hack, R. Ben Mahfoud, J. Melançon, A.D. Pelton, and S. Petersen: *Calphad*, 2002, vol. 26, pp.189-228.
- (12) T. Nishi and K. Shinme: *Tetsu-to-Tagané*, 1998, vol. 84, pp. 97-102.
- (13) H. Itoh, M. Hino, and S. Ban-ya: *Tetsu-to-Hagané*, 1997, vol. 83, pp. 623-28.
- (14) H. Itoh, M. Hino, and S. Ban-ya: *Tetsu-to-Hagané*, 1997, vol. 83, pp. 773-78.
- (15) M. Kowalski, P.J. Spencer, and D. Neuschütz: *Slag Atlas*, 2nd ed., Verlag Stahleisen GmbH, Düsseldorf, 1995.
- (16) *Steelmaking Data Sourcebook*, The Japan Society for the Promotion of Science, The 19th Committee of Steelmaking, Gordon and Breach Science Publications, New York, NY, 1988.
- (17) K. Suzuki, S. Ban-ya, and M. Hino: *Iron Steel Inst. Jpn. Int.*, 2001, vol. 41, pp. 813-17.
- (18) H. Ohta and H. Suito: *Iron Steel Inst. Jpn. Int.*, 2003, vol. 43, pp. 1301-08.
- (19) Z. Hong, X. Wu, and C. Kun: *Steel Res.*, 1995, vol. 66, pp. 72-76.
- (20) H. Ohta and H. Suito: *Metall. Mater. Trans. B*, 1996, vol. 27B, pp. 263-70.
- (21) S.R. Mehta and F.D. Richardson: *J. Iron Steel Inst.*, 1965, vol. 203, pp. 524-28.